Ecological Indicators 121 (2021) 107134

Contents lists available at ScienceDirect

Ecological Indicators

journal homepage: www.elsevier.com/locate/ecolind

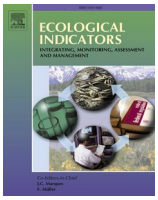

Analyzing the spatiotemporal dynamics of flood risk and its driving factors in a coastal watershed of southeastern China

Jianxiong Tang [a,b], Yanmin Li [c], Shenghui Cui [a,*], Lilai Xu [d,*], Yuanchao Hu [e], Shengping Ding [a], Vilas Nitivattananon [f]

[a] Key Lab of Urban Environment and Health, Institute of Urban Environment, Chinese Academy of Sciences, Xiamen 361021, China
[b] Xiamen Municipal Natural Resources and Planning Bureau, Xiamen 361012, China
[c] School of Geomatics, Anhui University of Science and Technology, Huainan 232001, China
[d] Institute for Disaster Management and Reconstruction, Sichuan University-The Hong Kong Polytechnic University, Chengdu 610207, China
[e] Research Center for Eco-environmental Engineering, Dongguan University of Technology, Dongguan 523808, China
[f] Urban Environmental Management, School of Environment, Resources and Development, Asian Institute of Technology, Bangkok, Thailand

ARTICLE INFO

Keywords:
Flood risk assessment
Spatial multi-criteria analysis
GIS
Spatiotemporal variation
Contribution analysis

ABSTRACT

Rapid urbanization and climate change can cause more extensive flood risk, in the absence of urgent and efficient adaptation measures. As the occurrence of floods varies with time and space, comprehensive and dynamical assessment of the spatiotemporal variability of flood risk and understanding of its drivers is vital for flood risk management. In this study, we developed a spatial multi-criteria analysis (SMCA) framework for quantifying the spatiotemporal dynamics of flood risk through a case study in a coastal watershed of southeastern China from 1990 to 2015. A comprehensive framework for flood risk assessment was constructed from the hazard, exposure, sensitivity and adaptive capacity components with 23 indicators. The results showed that the highest risk happened in the stage of 2006–2010, while the lowest risk stage was 2011–2015, with higher flood risk in the downstream areas of Jiulong River watershed (JRW). The contribution of each indicator reflects the difference in temporal, spatial and quantity aspects. The top 5 driving factors for JRW included: peak discharge, maximum daily rainfall, age structure, wetland, and reservoir. The risk perception showed a continuous growing impact on flood risk. However, some indicators only showed obvious contributions in the specified area: for example, the built-up expansion in Zhangzhou city; the increase of dike length and the improvement of dike standard in Xinluo district; and the increase of government financial investment in Zhangping and Liancheng district. This study demonstrates the well-performance of our proposed novel approach for flood risk assessment. Our results and conclusions are also of significance for policymakers to understand and point out the deficiencies in the current actions of flood adaption, and consequently develop more targeted and spatially-specific strategies for flood adaptation, in the context of climate change and rapid urbanization.

1. Introduction

Globally, climate-related disaster losses exceeded US$300 billion in 2017 (Swiss Re., 2017). Floods alone resulted in global losses worth US $60 billion in 2016 (Munich, 2017). China is the country that has suffered the most in both economic loss and human casualties as a result of flooding. From 2000 to 2017, the average annual number of people suffering from flood disasters in China was 127.46 million, including 1248 deaths, and the average direct economic loss due to flood accounted for 0.54 percent of GDP (China Flood and Drought Bulletin, 2017). Over the coming decades, flood risk is expected to continue increasing, due to the combined effects of climate change and socio-economic development (Field et al., 2012; UNISDR, 2011). The changes in rainfall patterns under climate change could result in increased frequency and severity of flood hazards (Aerts, 2018; Willner et al., 2018). The global population exposed to floods is expected to grow by a factor of three by 2050, because of the continued increase in population and economic assets in flood-prone areas, especially in Africa and Asia (Aerts, 2018; Jongman et al., 2012). Rapid urbanization can have both positive and negative effects on flood hazards. While engineering and other adaptive measures can help stabilize or even decrease the number of fatalities and the amount of direct damage, population

* Corresponding authors.
E-mail addresses: xmtangjx@163.com (J. Tang), shcui@iue.ac.cn (S. Cui), lilaixu@scu.edu.cn (L. Xu).

https://doi.org/10.1016/j.ecolind.2020.107134
Received 19 December 2019; Received in revised form 24 October 2020; Accepted 27 October 2020
Available online 28 November 2020

growth and the expansion of impervious surface areas increase sensitivity. Therefore, a comprehensive study on the mechanisms and factors that influence the dynamic temporal and spatial variations of flood risk is essential, and urgent, for flood disaster risk management in China, so that timely response plans and effective adaption strategies can be developed.

Flood risk refers to the probability of flood occurrence and its potential consequences and is thus a function of the hazard and the vulnerability of a receptor area that would be exposed to the hazard (Koks et al., 2015; Foudi et al., 2015; Chen et al., 2015). An increasing body of research has investigated the methods for evaluating flood risk. In general, the approaches can be divided into two types: qualitative and quantitative (Chen et al, 2015). Qualitative methods depend on expert opinions; these methods are widely used because they are simple and yet capable of functioning even with a scarcity of data (Furdada et al., 2008). Quantitative methods, on the other hand, are based on numerical expressions that can quantify the relationship between control factors and flood disaster risk (Wang et al., 2011), combining various data elements and producing comprehensive information about flood risk. The flood risk assessment requires a comprehensive consideration of the condition of the underlying surface (Ardıçlıoğlu and Kuriqi, 2019), the influence of the anthropogenic factor on the flood's seasonality (Ali et al., 2019a), the impact of seasonality in the flood's occurrence (Ali et al., 2019b), the impacts of floods in river geomorphology (Kuriqi et al., 2020), and the uncertainty in the dike design and operation during transient conditions (Kuriqi et al., 2016). Due to the scarcity of data and many uncertainties in the prediction of flood hazards and human activity, a comprehensive assessment of flood risk is full of challenges. The analytic hierarchy process (AHP) in multi-criteria decision-making (MCDM) is a semi-quantitative method based on multi-critical indexes; it organizes the relevant criteria into a hierarchical framework aimed at making a complex problem easy to analyze and manage (Saaty, 2008; Lyu et al, 2018). Furthermore, as there is spatial heterogeneity in social and economic development and natural conditions, GIS is an appropriate tool for processing spatial data along with attributes for deriving regional indicators of flood risk (Chau et al., 2013; Chen et al., 2015). Hence, spatial multi-criteria analysis (SMCA), which combines GIS and MCDM, is a suitable approach for flood risk analysis.

An increasing body of research concerning the flood risk assessment and management has applied the SMCA method in different research scales, and different types of flooding (fluvial, pluvial flooding or a compound thereof, or coastal flooding). Wang et al. (2011) designed a flood risk model in the Dongting Lake region, Hunan Province, China, the indicators included: hazards (rainfall, topography, vegetation cover, drainage network, downstream flood risk, flood control projects (dike density)), social sensitivity (population), economic sensitivity (cropland), and physical sensitivity (transportation). Dang et al. (2011) constructed a more sophisticated model for flood risk assessment in the Red River Delta, Vietnam; the indicators selected included: hazard (flood depth, flood duration, and flood velocity), economic sensitivity (total area of residential buildings, special-use buildings, public infrastructure, and agricultural areas), social sensitivity (population density, risk perception, spiritual values, and income levels), and environmental sensitivity (pollution, erosion, and open spaces). Yeganeh and Sabri (2014) selected distance from major streams and rivers, elevation, slope, land use, distance to discharge channels, and population as the criteria for generating a flood risk map in the Iskandar region of Malaysia. Martínez-Graña et al. (2016) present an analysis of the vulnerability (AVI Index) and hazard of flooding by sea-level rise (FRI Index) in the central Algarve (South Portugal), the vulnerability index was calculated using the following parametric thematic maps: lithology, geomorphology, slopes, elevations, distances, bathymetry, variations of the coastline, wave height and activity, variations of sea level and tidal range. Xiao et al. (2017) proposed a method to assess the flood hazard risk in the Han River region, Hubei province, China; the indicators included: topographical (elevation, slope), hydrological (flow accumulation, soil conservation service curve number, topographic wetness index, distance to the river), and flood-resistance (dikes, pumping stations). Lyu et al. (2018) presented an integrated assessment model for flood risk in the Guangzhou metro system; the indicators included: hazards (rainy season, average rainfall, the average number of rainy days), exposure (elevation, slope, river proximity, river density), and sensitivity (land use, metro line proximity, metro line density, road network proximity, road network density).

Although the selected indicators cover many aspects and their classification differed in previous studies, few studies fully considering the indicators among flood hazard, exposure, sensitivity, and adaptive capacity, thereby possibly producing unreliable flood risk maps. In particular, studies that considering personal sensitivity (perception of flood risk) and flood adaptive capacity – which includes both engineering measures (e.g., dike lengths and standards, reservoirs) and non-engineering measures (e.g., wetlands, vegetation, and financial investment) – have been rare. In addition, flood risk is dynamically changing with the progression of climate change and rapid urbanization. Yet precious researches have usually selected average precipitation data during a historical period or precipitation under future climate change scenarios for flood hazard assessment, land use data, or the socio-economic condition at a certain time for exposure or sensitivity assessment, and there has been little research analyzing dynamic flood risk variations and exploring the respective contribution of each driving factor in a series of historical periods. All of this evidence indicates that the existing SMCA flood risk assessment framework is not comprehensive and that it needs to be expanded and improved, applied to the dynamical assessment of flood risk variations.

To address this deficiency, the present study aims to: (1) develop a comprehensive framework for flood risk assessment with SMCA, integrating a wide range of indicators across hazard, exposure, sensitivity, and adaptive capacity; (2) dynamically review the flood risk evolution during study periods and quantify the relative contribution of each factor in JRW. The results could provide policymakers with the information that they need, to develop more comprehensive and spatially-specific strategies for flood risk adaption.

2. Materials and methods

2.1. Study area

The JRW covers approximately 14,700 km^2 in southeastern China (from 116°46′55″ E to 118°20‘17“E and from 24°23‘53” N to 25°53’38” N) and is the second-largest watershed in Fujian province. The watershed contains nine counties or districts—Xiangcheng, Longwen, Xinluo, Zhangping, Hua'an, Changtai, Pinghe, Longhai, and Nanjing – with 88.26% of it located in Zhangzhou and Longyan cities. It is situated in a subtropical zone with a monsoon climate: the annual average temperature is 19–21 °C, and annual precipitation averages 1400–1800 mm, of which 70% occurs between April and September (Huang et al., 2014). The river basin is composed of three main streams: the North river, comprising the upper reach of the watershed, and the West and South rivers, in the lower reach. The North and West rivers' confluence is located in Xiangcheng, then they merge with the South River in the Longhai district, and finally flow into the Jiulong River estuary and the western Xiamen Sea, as depicted in Fig. 1.

More than 3.8 million people live in the JRW, and the GDP of the area accounts for a quarter of Fujian Province's economic output (Huang et al., 2012). Rapid urbanization in JRW has gone hand in hand with rapid population growth, socio-economic development, an increase in the built area and massive investment in the construction of infrastructure. According to the statistical yearbooks of Longyan and Zhangzhou cities, the urbanization rate increased by 38.1% and 39.7% in Zhangzhou city and Longyan city, respectively, between 1980 and 2015. The combined effects of these increased stresses in the region indicate that evaluating the flood risk variations and exploring their

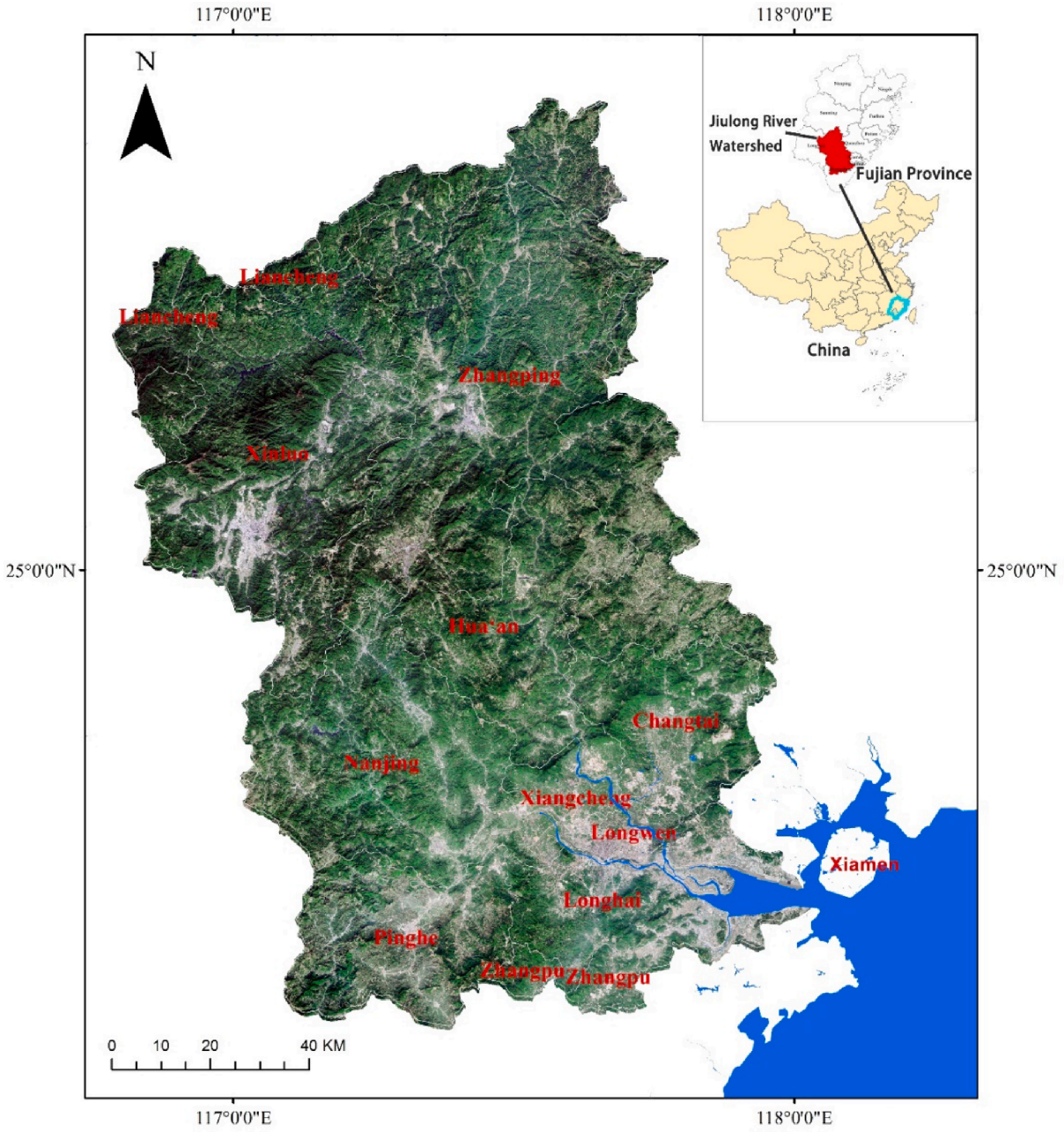

Fig. 1. Study area.

main driving forces are of the utmost importance.

2.2. Framework for flood risk assessment

In this study, a spatial multi-criteria analysis and evaluation framework based on AHP was developed to describe the flood risk variation in the case study area. Fig. 2 shows the conceptual framework for flood risk variation assessment, the framework consists of three parts: (1) flood risk assessment index system, (2) calibration procedure incorporated into GIS, and (3) contribution analysis.

2.2.1. Risk assessment model

To evaluate the flood risk variation in the JRW, first, the flood risk of each stage was assessed, then the changes in historical flood risk were determined, and finally, the contribution of each component and indicator to flood change was explored. The detailed procedure is shown in Text S1, Fig. S1 (SI).

The risk of a flood disaster is associated with the factors of hazard, exposure, sensitivity, and adaptive capacity, the formula for calculating the flood riks is defined in Eq. (1), the explanation of it is shown in Text S2 (SI):

$$Flood\ risk = Hazard + Exposure + Sensitivity - Adaptive\ capacity \tag{1}$$

Flood risk means the interactive results of hazard, exposure, sensitivity, and adaptive capacity indexes, which can be expressed by Eq. (2):

$$Risk = \left(\sum_{i=1}^{n} h_i H_r\right)_{Hazard} + \left(\sum_{j=1}^{n} e_j E_j\right)_{Expoure} + \sum_{k=1}^{n} (s_k S_k)_{Sensitivity} - \sum_{l=1}^{n} (a_l A_l)_{adptive\ \ capacity} \tag{2}$$

where i, j, k, and l are the sequence numbers of the hazard, exposure,

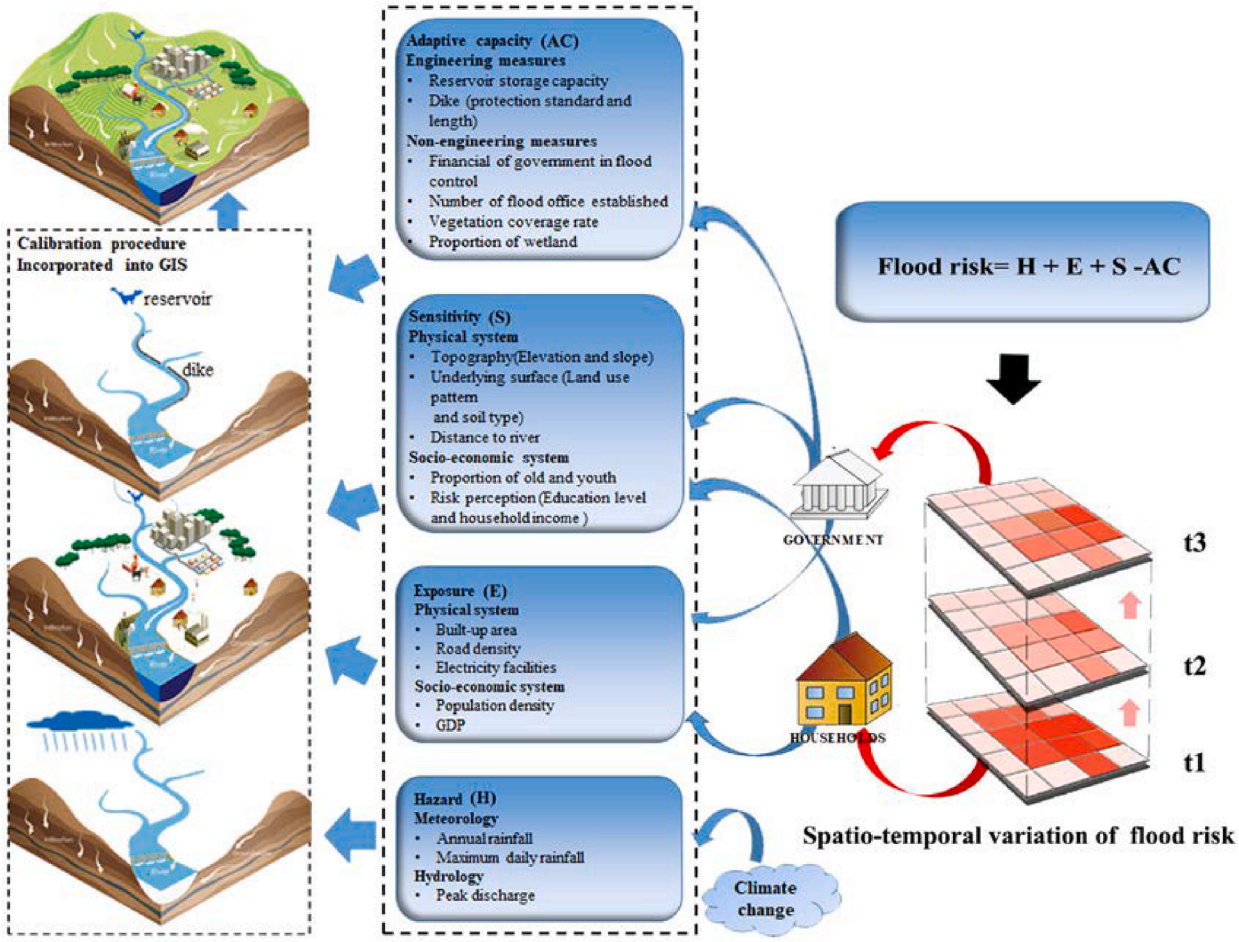

Fig. 2. Overview of the conceptual framework for flood risk variation assessment. Flood risk is a function of the hazard, exposure, sensitivity, and adaptive capacity, and indicators among each component are selected. As climate change can influence hazard, the behavior of government and households can influence the exposure, sensibility, and adaptive capacity, flood risk is dynamically changing.

sensitivity, and adaptive capacity indexes, respectively; h_i, e_j, s_k, and a_l are the weights of the four components, respectively; and H_i, E_j, S_k, and A_l are the normalized values of the indexes related to the four components, respectively.

2.2.2. *Index system*

To construct a scientific, comprehensive, reasonable and practical flood risk assessment index system, the following principles should be followed: (1) The selected indicators should effectively reflect the essential characteristics of the flood disaster; these can be quantitative or semi-quantitative; (2) The indicator should be spatialized as much as possible, to reflect the spatial distribution pattern of regional flood risk; thus the fuzzy flood risk can be quantified and visualized; (3) As the indicators cover many fields, the availability of data is an important criterion for selecting indicators. The index system consists of three layers: object layer, index layer, and sub-index layer. The object layer is the flood risk of the JRW, labeled as I. The index layer includes four categories: hazard, exposure, sensitivity, and adaptive capacity, labeled as I_1, I_2, I_3, and I_4, respectively. The sub-index layer covers 23 sub-indexes that correspond to the hazard, exposure, sensitivity, and adaptive capacity components. The description of the chosen indicators is shown in Table S1 (SI).

(1) Hazard index

The hazard index was chosen to represent the characteristics of a combination of fluvial and pluvial flood hazards. The peak flow recorded by hydrological stations can directly reflect the degree of a fluvial flood. However, as there didn't exist enough record data for the measurement of pluvial floods in the watershed scale, rainfall data is the alternative. As is known to all, the short-term heavy rainfall is most likely to cause both fluvial and pluvial flooding, meanwhile, lower-intensity rainfall can also induce flooding when the ground is saturated. Considering the availability of data, the annual rainfall (I_{11}) and the maximum 24-h precipitation of each year (I_{12}) was used to represent the rainfall hazard, and the maximum flood discharge of each year (I_{13}) was used to represent the hydrological hazard. As the frequency and intensity of the rainfall and peak flood discharge are different in each area, the critical hazard value of precipitation and flood are described by the return period. The detailed information is shown in Table 1, the spatialization approach for hazard indexes is introduced in Text S3 (SI).

(2) Exposure index

Exposure refers to the amount and degree of the disaster-bearing body (people, property, buildings, etc.) exposed to the disaster. Considering the data availability, from the system perspective, this framework summarizes the watershed as a comprehensive disaster-bearing body composed of a physical subsystem and a socio-economic subsystem. In the physical subsystem, built area (I_{21}), road density (I_{22}), and electrical facility density (I_{23}) were selected as the representative indexes. In the socio-economic subsystem, GDP (I_{24}) and population density (I_{25}) were selected as the representative indexes. The spatialization approach for exposure indexes is introduced in Text S4 (SI).

Table 1
Quantification for precipitation and peak flow by return period.

Return period (year)	0–2	3–5	6–10	11–20	21–30	31–50	51–100	101–200	201–500
Level value	1	2	3	4	5	6	7	8	9

(3) Vulnerability index

Vulnerability refers to the degree of loss or injury due to potential risk factors in a given hazardous area. The lower the vulnerability of the disaster-bearing body, the smaller the disaster risk, and vice versa. Corresponding to the above exposure index, the vulnerability index chooses the sub-indexes from the physical and socio-economic subsystems. It is commonly recognized that a low-lying area is more vulnerable to flooding than is a higher area, that the area closest to the river is most vulnerable to flooding, and that the steeper the terrain slope, the lower the hazard of an area (Wu et al., 2015). In addition, the runoff conditions and infiltration capabilities of different underlying surfaces vary considerably. Thus, the distance to the river (I_{31}) was selected, and DEM (I_{32}) and slope (I_{33}) were used to represent topography, and land use pattern (I_{34}) and soil type (I_{35}) to represent the underlying surface area; these were selected as sub-indexes to describe the vulnerability level of the physical system. When considering the vulnerability of the socio-economic system, youth and the elderly are considered more vulnerable when flooding occurs, and thus the proportion of children and the elderly (I_{36}) was selected. Furthermore, as risk perception is positively correlated with educational level and household income, the proportion of highly educated people within the population (I_{37}) and the household income per capita (I_{38}) were selected to represent risk perception. The spatialization approach for sensitivity indexes is introduced in Text S5 (SI).

(4) Adaptive capacity index

The flood adaptive capacity includes both engineering and non-engineering measures. Even though engineering means are important, non-engineering measures should not be ignored. The higher the resilience, the smaller the potential loss and risk. The reservoir capacity (I_{41}) and dike values were used to represent engineering protection measures (the dike value is a compound of the dike length (I_{42}) and dike standard (I_{43})). The proportion of wetland (I_{44}), vegetation cover rate (I_{45}), financial investment (I_{46}), and the number of organizational personnel in the flood protection department (I_{47}) were used to represent non-engineering protection measures. The reprehensive indicators far beyond mentioned above, some import indicators (e.g. the urban drainage network density) aren't included in the current study mainly because of the data available in such watershed-scale study. The spatialization approach for hazard indexes is introduced in Text S6 (SI).

2.3. Criteria normalization

As different criteria have different ranges and dimensions, to facilitate the comparisons among various indexes, the value of each sub-indicator was normalized over the range from zero to one (Lai et al., 2015; Lyu et al., 2018), these are expressed as Eqs. (3) and (4):

$$r_{ij} = \frac{X_{ij} - X_j^{min}}{X_j^{max} - X_j^{min}} \tag{3}$$

$$I_{ij} = \frac{X_j^{max} - X_{ij}}{X_j^{max} - X_j^{min}} \tag{4}$$

where I_{ij} is the normalized value for the raw value of the ith district of the j-th criterion: X_j^{max} and X_j^{min} respectively refer to the maximum and minimum values of the j-th criterion. Eq. (3) is suitable for positive criteria, Eq. (4) for negative criteria, meaning that the flood risk will decrease with an increase in the value. In the assessment index system, the following sub-indexes were negative factors: I_{31}, I_{32}, I_{33}, I_{37}, I_{38}, I_{41}, I_{42}, I_{43}, I_{44}, I_{45}, I_{46}, I_{47}; all the other sub-indexes were positive.

2.4. Weight calibration

To aggregate the criteria, one of the most important steps is to generate criteria weights. The analytic hierarchy process (AHP) is a commonly used method for the quantitative analysis of indicators. The main idea of AHP is to rely on the experience of many experts in related fields to compare, judge, and assign each factor, to obtain a judgment matrix. In a judgment matrix, the relative importance of each indicator is defined as an exact integer between 1 and 9, then the value of the consistency ratio (CR) is used to evaluate the sensitivity and consistency of the judgment matrix. If CR < 0.1, then the judgment matrix is reasonable. (Saaty, 1977). In this study, 72 questionnaires were distributed to experts from different departments: 30 to scientific research departments (researchers), 22 to water conservation departments (government managers), and 20 to water conservation design institutes (engineers), and the comparative weights of various indicators were obtained through the Yaahp software.

2.5. Contribution analysis

The relative contributions of the hazard, exposure, vulnerability, and adaptive capacity components were quantified according to the process defined in previous literature (Vousdoukas et al., 2018). The first step is to estimate the relative change (RC) of each component in each stage. The RC of the hazard component, for example, is given by Eq. (5):

$$RC_{Hazard} = \left[\frac{R_{Hazard,\ Stage}}{R_{Baseline}} - 1\right] \tag{5}$$

where R is the flood risk, $R_{Baseline}$ is the flood risk for 1990, and $R_{Hazard,Stage}$ is the flood risk considering only the dynamics in the hazard component (and the static exposure, vulnerability, adaptive capacity components). The relative contribution of each component is then obtained as the ratio of its RC is divided by the sum of the absolute values of all the components. The relative contribution of hazard component is then given by Eq. (6):

$$\rho_{Hazard} = 100 \times \left[\frac{RC_{Hazard}}{|RC_{Hazard}| + |RC_{Exposure}| + |RC_{Sensitivity}| + |RC_{Adaptive\ capacity}|}\right] \tag{6}$$

where ρ_{Hazard} refers to the relative contribution of hazard component; RC_{Hazard} refers to the relative change of hazard component; the $|RC_{Hazard}|$, $|RC_{Exposure}|$, $|RC_{sensitivity}|$, and $|RC_{Adaptive\ capacity}|$ refer to the absolute value of relative change of hazard, exposure, sensitivity, and adaptive capacity components. The relative contributions express the relative importance of each component and indicator to flood risk change. The same approach was followed to assess the relative contributions of each indicator to the total flood risk in each stage.

3. Results

3.1. Criteria of weight analysis

Based on the flood risk assessment framework and the AHP method, the weight of each indicator was obtained, and the results are shown in Table S2 (SI). The consistency ratio (CR) of the pairwise comparison

matrix is calculated as 0.0055 < 0.1. So the weights are shown to be consistent and they are used in the selection process. In the target layer, the weights of the components are shown as: hazard (0.5411) > adaptive capacity (0.202) > sensitivity (0.1912) > exposure (0.0657); in the index layer, as: hydrology (0.4638) > sensitivity of physical system (0.1275) > engineering measures (0.101) = non-engineering measures (0.101) > meteorology (0.0773) > sensitivity of socio-economic system (0.0637) > exposure of physical system (0.0329) > exposure of socio-economic system (0.0328); in the sub-index layer, as: peak discharge (0.4638) > maximum daily rainfall (0.0663) > distance to river (0.0524) > wetland proportion (0.0508) > reservoir capacity (0.0505) = dike (0.0505) > proportion of old and youth (0.0455) > land-use pattern (0.036) > > financial investment (0.0239) > soil type (0.0256) > built-up area (0.0236) > GDP per capita (0.0164) = population density (0.0164) > vegetation cover rate (0.0148) > number of flood control offices established (0.0116) > annual rainfall (0.011) > household income (0.0091) = education level (0.0091) > elevation (0.0078) > road density (0.0064) > slope (0.0058) > electrical facility density (0.0029).

3.2. Analysis of flood hazard component

The spatial and temporal evolution of the hazard from 1990 to 2015 as shown in Fig. 3. First, the hazard fluctuated during these periods, it was obvious in Zhangzhou city, and the hazard was highest from 2006 to 2010 (Fig. 3(e)) compared to the other periods; second, the hazard in the downstream districts was higher than in the upstream districts, especially obvious in Zhangping, Hua'an, Changtai, Longwen, and Xiangcheng districts. Several reasons were responsible for these, first, the maximum rainfall during these 25 years fluctuated, and the volatility of maximum rainfall was highest in 2005 and 2006, most obvious in Changtai district; second, as Zhangping and Hua'an district located at the downstream of the North River, Xiangcheng and Longwen districts located at the confluence of West River and North River, therefore, the recorded peak flood flows in these districts were higher and also fluctuated more than the others.

3.3. Analysis of exposure index

As shown in Fig. 4, exposure has increased greatly in the JRW during the most recent 25 years. From 1990 to 2000, the exposure grew slowly, while the watershed developed rapidly after 2000, especially in the Xinluo district, which is located in downtown Longyan city, and in the Xiangcheng, Longwen, and Longhai districts, which are located in downtown Zhangzhou city, southeast of the JRW. Several causes are responsible for this phenomenon: first, urbanization has resulted in rapid increases within the physical system during these 25 years (the built area has increased by a factor of 60, the road density by about 116%); second, the socio-economic capacity has also grown rapidly during these 25 years: the average annual GDP growth rates in Zhangzhou and Longyan cities were 5.25% and 3.04%, respectively, and the average population density increased by a factor of about 9.

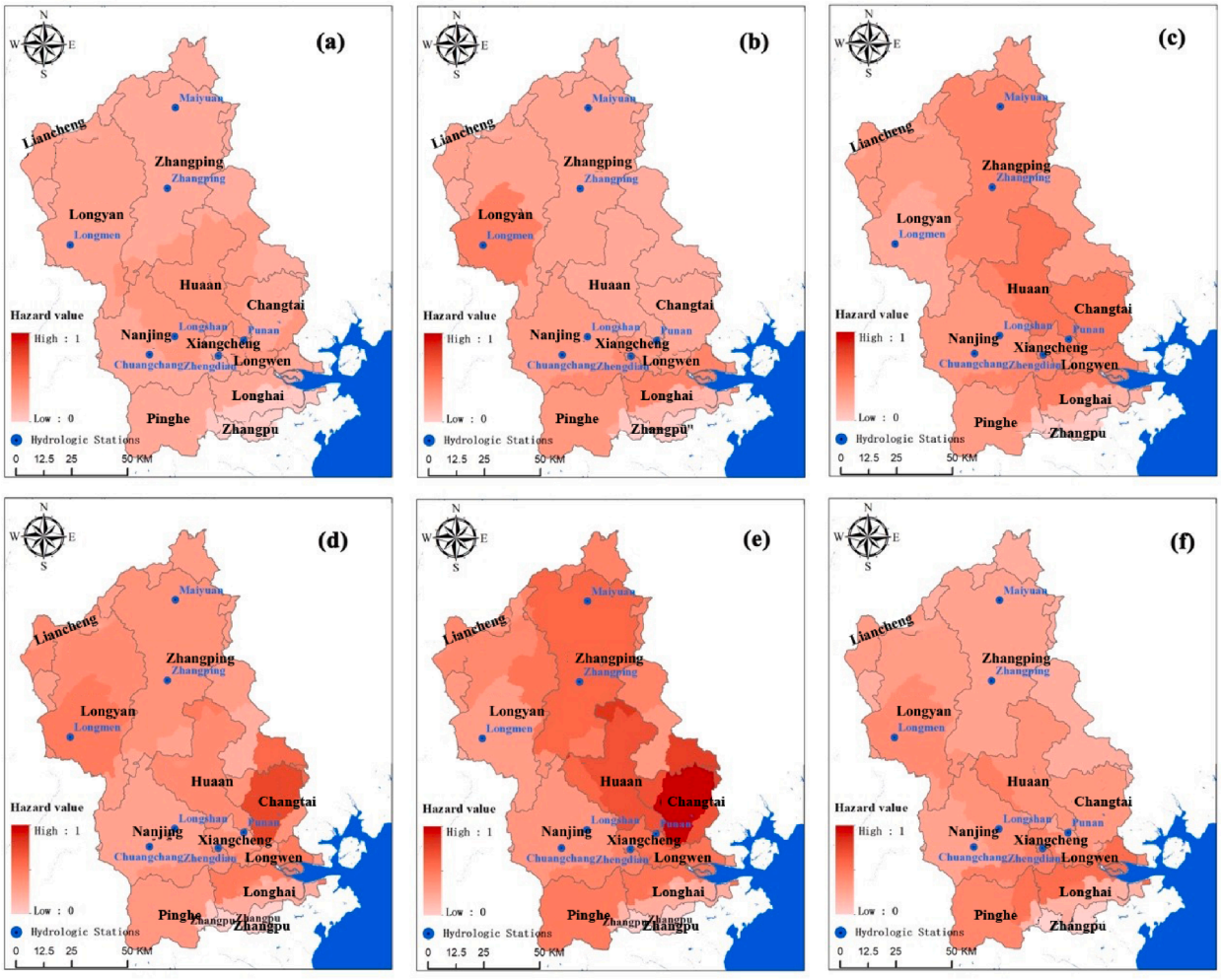

Fig. 3. Spatial distributions of hazard values from 1990 to 2015: (a) 1990; (b) 1991–1995; (c) 1996–2000; (d) 2001–2005; (e) 2006–2010; (f) 2011–2015.

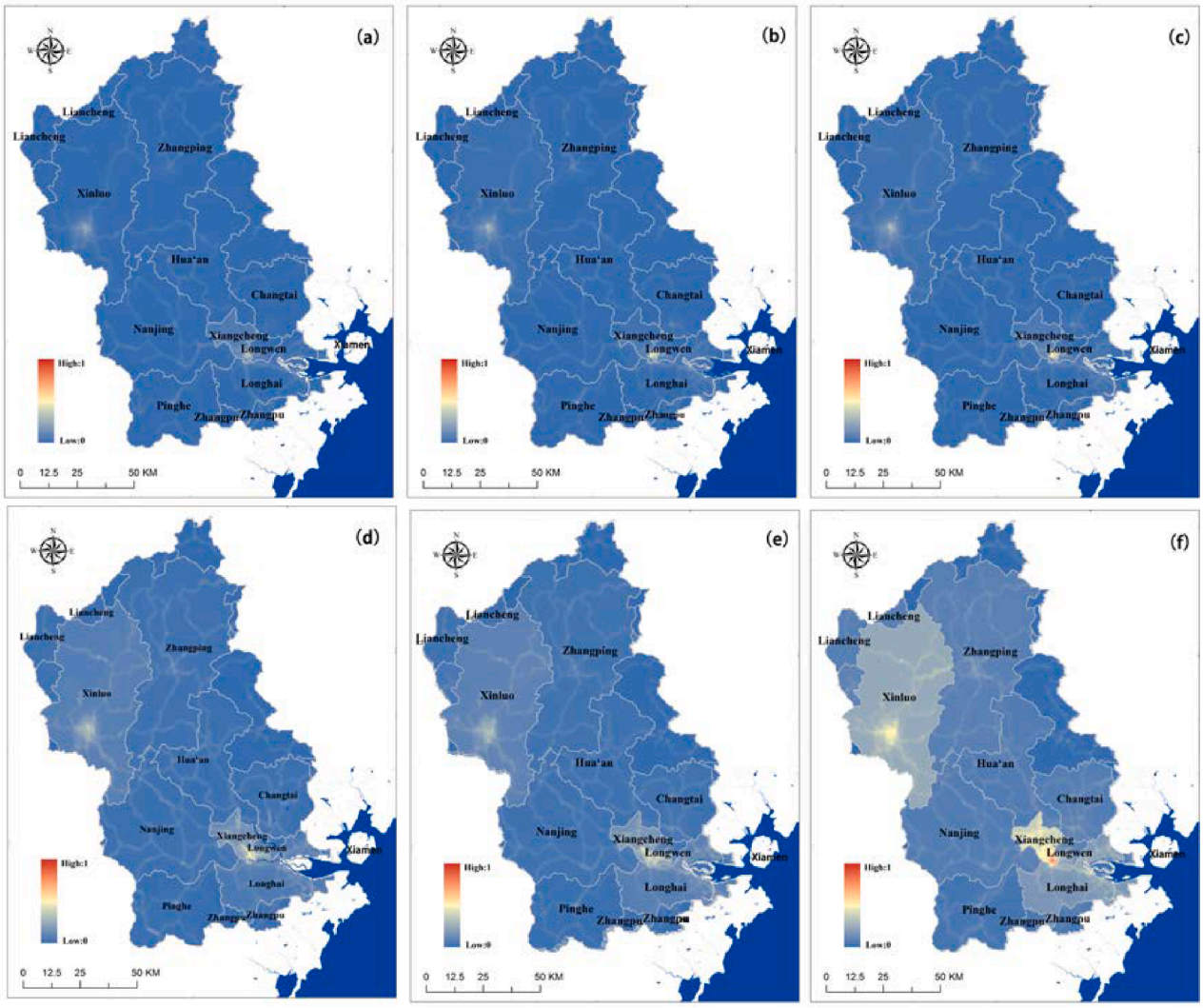

Fig. 4. Spatial distributions of exposure values from 1990 to 2015: (a) 1990; (b) 1991–1995; (c) 1996–2000; (d) 2001–2005; (e) 2006–2010; (f) 2011–2015.

3.4. Analysis of sensitivity index

Fig. 5 shows the spatial distribution and evolution of sensitivity in the JRW during 1990 and 2015. As shown in Fig. 5, the sensitivity during this period was diminishing; the highest sensitivity stage is shown in Fig. 5(a), and the lowest sensitivity stage in Fig. 5(f), and the highest sensitivity area was located in downtown Zhangzhou city. Furthermore, the downstream stretch of the watershed was more vulnerable than the upstream one, and the urban area and the region nearby the river were higher than the others. Several causes are responsible for these values: first, the rapid increase in the built area caused by urbanization increased the impervious surface area; secondly, the flood risk perception of the residents in the JRW had improved greatly, due to the increased educational and household income levels, and it helped lower the sensitivity; thirdly, as the downstream districts are located in a low-lying area, the vulnerabilities are higher there than in the upstream districts, in terms of topography.

3.5. Analysis of adaptive capacity index

Fig. 6 shows the spatial evolution of the flood adaptive capacity in the JRW from 1990 to 2015. It is easy to see that the adaptive capacity of the watershed had improved a great deal during these years. As shown in Fig. 6(a), the adaptive capacities of the Xiangcheng and Longwen districts located in the downtown of Zhangzhou city were stronger than those of the other districts. However, during stage and b, the adaptive capacity of the Xinluo and Nanjing districts caught up, because of the Wan'an reservoir in the Xinluo district and Nanyi reservoir in the Nanjing district had been built and put into use in 1991 and 1995, respectively. The adaptive capacity of every district in the watershed has improved in various degrees since then, with the improvement of the Xinluo district being higher than that of other regions in the basin. Several causes can be found for these results. First, the economy had improved greatly during this period; secondly, great importance had been attached to flood control by the local government, especially in Longyan city.

3.6. Analysis of integrated flood risk and contributions of indicators

After combining the values of the hazard, exposure, sensitivity, and adaptive capacity components, the flood risk value for each historical stage was calculated; the results are shown in Fig. 7. In general, the flood risk in the downstream stretch of the JRW (especially the southeast coastal area) was higher than in the upstream stretch, and among all the stages, the flood risk during 2006–2010 was the highest, and that during 2011–2015 the lowest.

The contribution of each component and indicator was analyzed in detail by the methods mentioned in Section 2.5. Fig. 8 shows the contribution analysis result of each component (hazard, exposure, sensitivity, and adaptive capacity) relative to the base year (1990) each

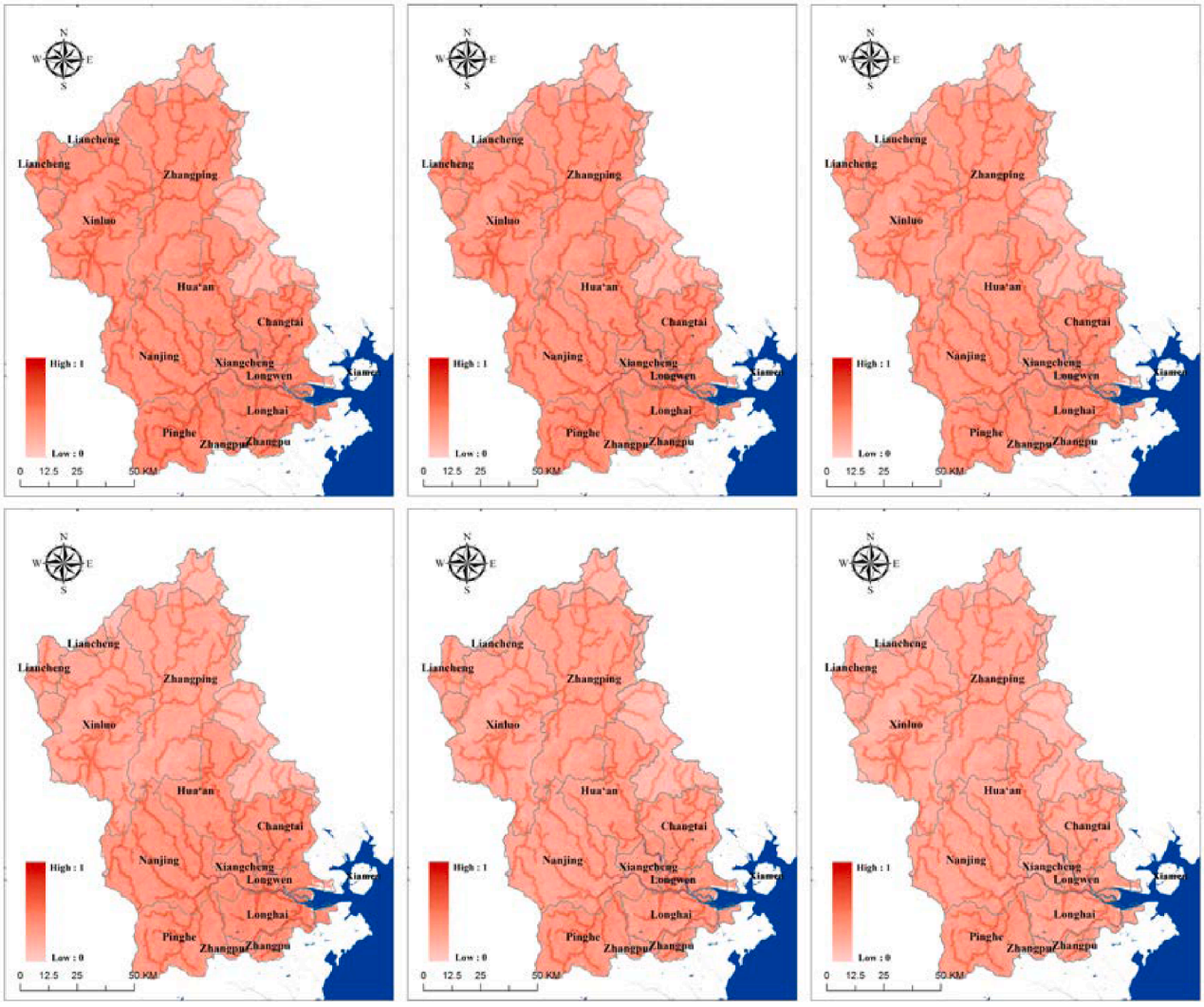

Fig. 5. Spatial distributions of sensitivity values from 1990 to 2015 in the JRW: (a) 1990; (b) 1991–1995; (c) 1996–2000; (d) 2001–2005; (e) 2006–2010; (f) 2011–2015.

stage. Fig. 9 shows the contribution analysis result of the top 4 indicators during different stages in different districts, relative to the base year (1990), and the detailed contribution of each indicator was shown in Fig. S2 (SI). As shown in Fig. 8, first, although the contribution of each component varied across districts, the order of the contributions in most districts was: hazard > adaptive capacity > sensitivity > exposure; secondly, as the climate changed randomly, the hazard contribution fluctuated; thirdly, the adaptive capacity showed a negative contribution to flood risk in most districts except for Xiangcheng and Longwen in Zhangzhou city. Due to the differences in socio-economic state and natural conditions, the degree of contribution of each indicator to flood risk also showed spatial heterogeneity, and therefore, it is necessary to explore the contribution of each driving factor that leads to a change in the flood risk in each district. In Fig. 9, the results show that, first, the contribution of the top 5 main driving factors varied with space and time, the main driving indicators in the whole watershed on average included: maximum daily rainfall, peak discharge, age structure (the proportion of elderly and youth), wetland and reservoir, second, as flood control projects developed rapidly during 1990–2015 in Xinluo, Nanjing and Hua'an districts, the reservoir and dikes emerged as the main driving factors in these districts during the period; third, with rapid urbanization, the increase in the built area has shown an obvious contribution to flood risk evolution in Xiangcheng (downtown of Zhangzhou City) and Xinluo (downtown of Longyan City) districts, especially during period from 2011 to 2015, as shown in Fig. S4 (SI); fourth, the decrease in wetland area showed a significant contribution to flood risk variation in the Xiangcheng and Longwen districts during the process of rapid urbanization, as shown in Fig. S3 (SI); fifth, as the local governments attach different importance to flood financial investment and thus resulting in varying degrees of impact on flood risk evolution. What's more, Fig. S5 (SI) showed that the risk perception (represented by household income and education level) contributed a lot in most districts from 2011 to 2015, and this was the result of the rapid development of socio-economic and lower contribution of hazard indicators during that period.

4. Discussion

4.1. Applicability of the present approach

Flood damages have increased significantly and are expected to rise in many parts of the world due to climate change and urban expansion, especially in developing countries that often lack sufficient technical and financial capabilities (Thieken et al., 2016). Furthermore, flood risk is a geographically and socially differentiated, spatially heterogeneous, dynamic, and complex combination of interactive processes (Balica et al., 2009; Chang and Chen, 2016). It is vital, therefore, to study the mechanisms and factors that influence the temporal and spatial variations of

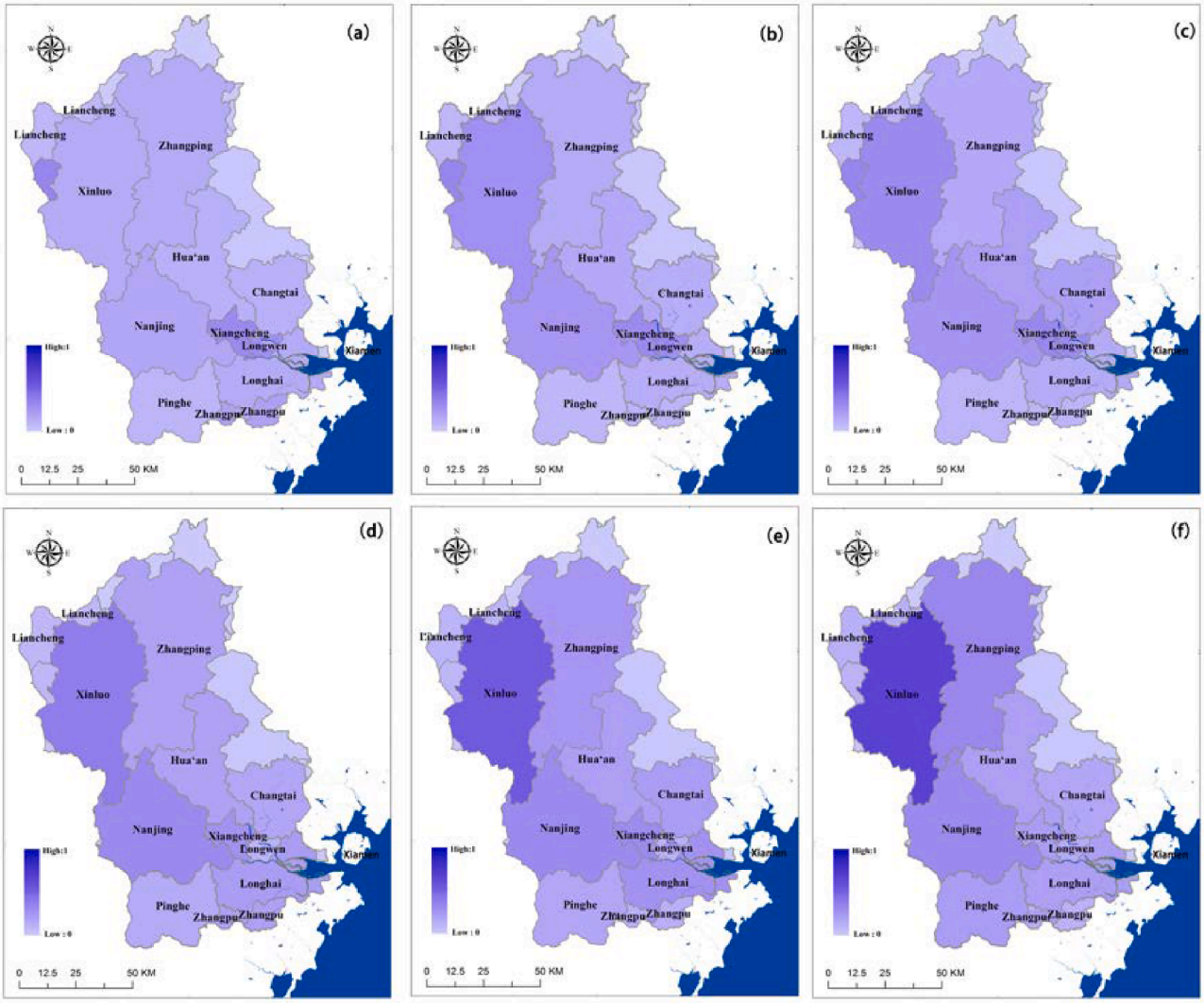

Fig. 6. Spatial distributions of flood adaptive capacity from 1990 to 2015: (a) 1990; (b) 1991–1995; (c) 1996–2000; (d) 2001–2005; (e) 2006–2010; (f) 2011–2015.

flood risk, and accordingly, specific locally appropriate and efficient adaptation measures considering spatial heterogeneity should be taken by policymakers. In this study, we have presented a comprehensive approach which integrated climate variability, environmental change, and human activity to assess the temporal and spatial evolution of flood risk in JRW, and furtherly investigated the relative contribution of each component and indicator to flood risk evolution.. The indicators involved in this approach include (1) hazard indicators from meteorology and hydrology; (2) exposure indicators from the physical and social-economic systems; (3) sensitivity indicators from the environmental and socio-economic systems; and (4) adaptive capacity indicators from both engineering and non-engineering measures. Meanwhile, the data included in the flood risk assessment framework are universal, and the contribution of each component and indicator to flood risk evolution has been analyzed in detail, therefore, the approach can be easily applied to other watersheds. In addition, the indicators are not limited as described in this paper but can be expanded according to the individual study and data accessibility. Furthermore, the approach is not only limited to historical flood risk assessment but can also be extended for future flood risk evolution or other types of disaster risk. Above all, as flood risk is driven by a combination of interactive processes, and is dynamic and spatially heterogeneous, the approach may help understand perspectives for future adaption by considering the feedback mechanisms between the drivers of flood risk change in the past.

4.2. Comparative contributions of flood hazard, exposure, sensitivity, and adaptive capacity

The factors studied, and the mechanisms whereby they influence flood risk evolution, are diverse and complex because they can come from different sources such as meteorology, hydrology, terrain, land use, and socio-economic and flood control measures. Furthermore, with climate variability, environmental change and economic and social development in flood-prone areas, it's worth noting that the flood risk is not static but dynamic and spatial heterogeneity. In terms of this puzzle, policymakers need to develop methods for quantitatively assessing flood risk, and explore the driving factors for flood risk evolution. This study not only employed a wide range of indicators among hazard, exposure, sensitivity, and adaptive capacity components to assess the historical flood risk in JRW but also compared the respective contributions of each indicator to flood risk dynamics. The results in this study demonstrate that the maximum daily rainfall, annual rainfall, peak discharge from hazard component, and reservoir, dike from the adaptive capacity component, are the most significant driving factors among the whole watershed, and the other indexes, such as household income, financial investment, age structure, built-up area, and wetland area, have an obvious effect on flood risk change in some districts. Therefore, to make flood mitigation and adaption measures more efficient and targeted, decision-makers should fully consider the factors that might influence

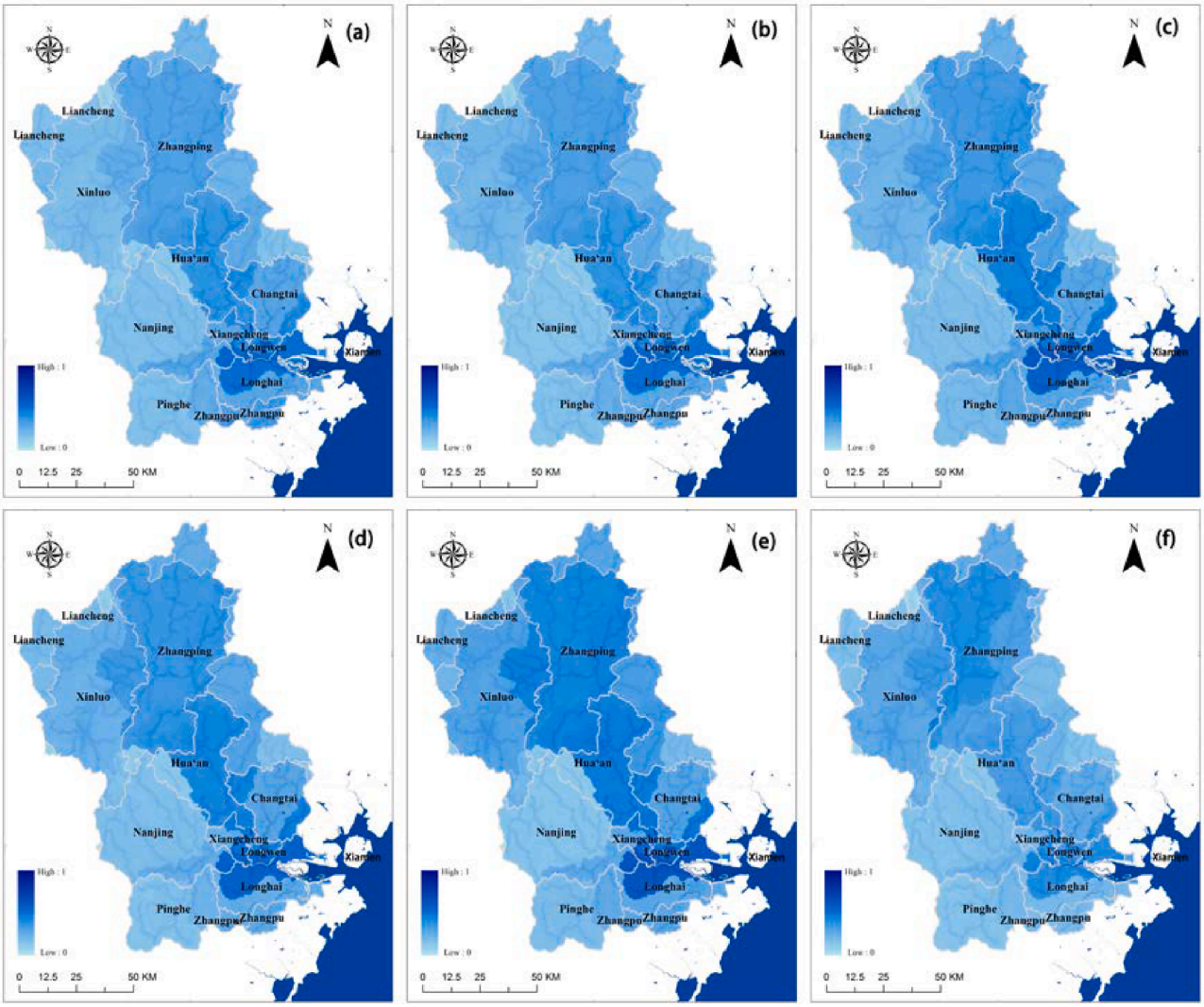

Fig. 7. Spatial distributions of historical flood risk from 1990 to 2015: (a) 1990; (b) 1991–1995; (c) 1996–2000; (d) 2001–2005; (e) 2006–2010; (f) 2011–2015.

flood risk based on local realities.

The results in this study reveal that the flood risk in the downstream stretch of the river is higher than that in the upstream stretch. As demonstrated by the analysis of the contributions to the flood risk variation, the hazard indexes (maximum daily rainfall, annual rainfall, peak discharge) were the most significant in most districts, a result consistent with previous research on a flood risk assessment which concluded that the hazard index was the most significant among the three indexes of hazard, exposure, and sensitivity (Sadiq and Tesfamariam, 2009; Liu et al., 2016). Nevertheless, the results also demonstrate that the sensitivity and adaptive capacity indexes also contribute a great deal to the flood risk variation. In terms of the sensitivity indexes, this study has integrated human behavior into flood risk assessment, and existing risk assessment methods rarely include this critical factor (Aerts et al., 2018; Bodoque et al., 2019). In addition, the results reveal that improving the educational level and household income also improves the social perception of flood risk and thus lowers the sensitivity, and this result is also in line with previous studies (Armaş and Avram, 2009; Lin et al., 2018). In terms of the adaptive capacity indexes, this study has revealed that flood protection engineering measures (dikes, reservoirs) vary greatly across different regions, and they had contributed the most to the flood risk variation in Xinluo district, this result may suggest that the political attitudes toward flood protection investment are spatially heterogeneous, a finding consistent with previous studies (Jongman et al., 2015; Willner et al., 2018). Although the engineering protection measure indexes are the primary adaptive-capacity ones, the contribution of the non-engineering protection measures should not be underestimated, and this study has revealed that the degeneration of wetlands due to human activity made an obvious contribution to the flood risk in the Longwen district.

Although the results in this study show that exposure contributed the least to the flood risk variation, the contribution of the built area and road density factors to the flood risk variation was especially apparent in urban areas (Xiangcheng and Xinluo districts). The rapid increase in the built area caused by urban sprawl increased the flood exposure, and along with urbanization comes underlying surface changes which increase the runoff coefficient, and result in a further increase in sensitivity; this result corresponds with that in a previous study (Kundzewicz et al., 2018).

4.3. Implications

Both previous research and this study show that changes in the hazard indexes contribute the most to the change in flood risk. In the context of climate change, a great deal of research has pointed out that future increases in flood frequency and severity due to changes in extreme weather can be expected (Field et al., 2012; Visser et al., 2014), and absolute damage may increase by up to a factor of 20 by the end of

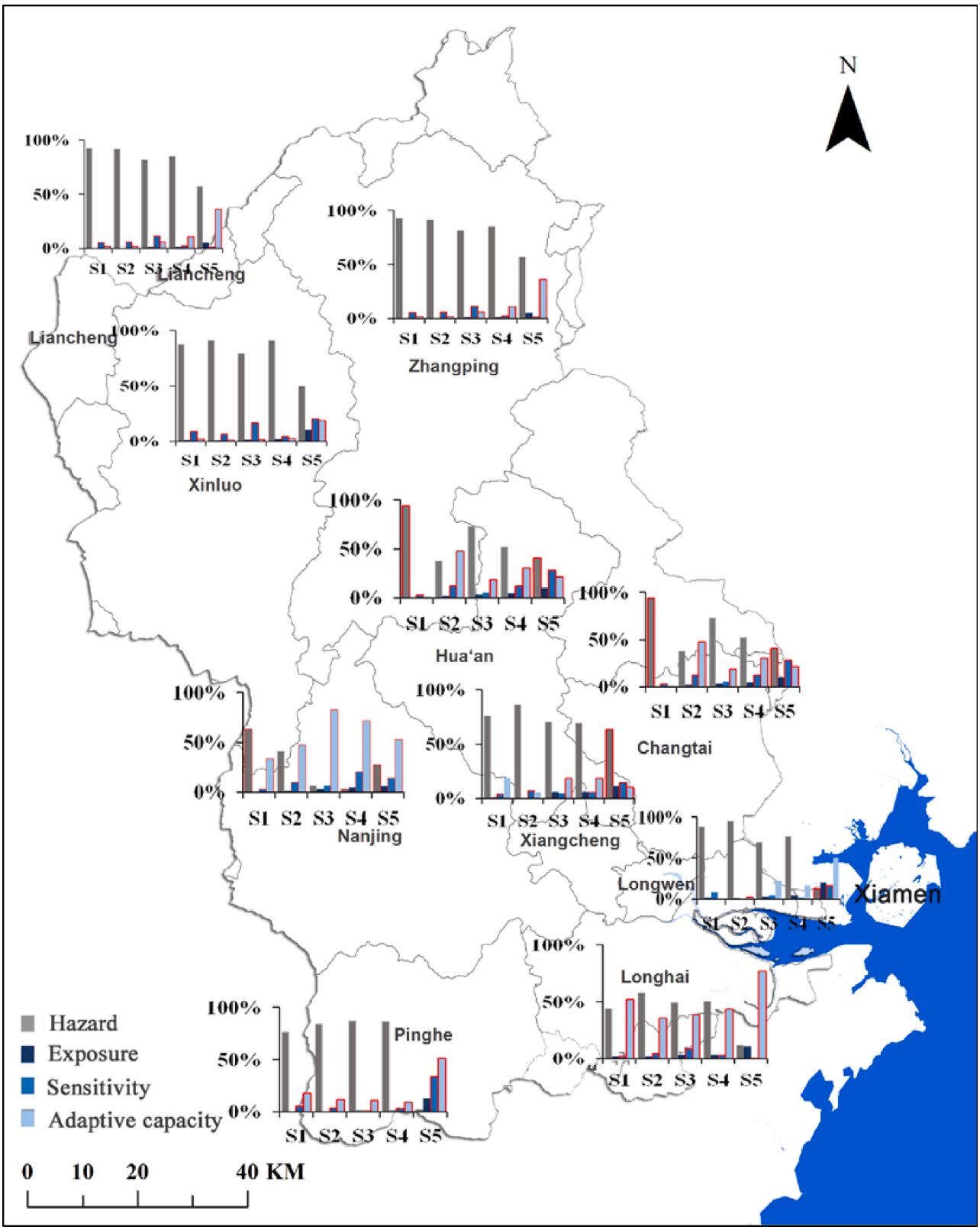

Fig. 8. Contribution of each component in each stage compared to the base year (1990). S1 refers to the stage 1991–1995, S2 to the stage 1996–2000, S3 to the stage 2001–2005, S4 to the stage 2006–2010, and S5 to the stage 2011–2015. (The red board line means the negative contribution).

the century, without action (Winsemius et al., 2016). Furthermore, rapid urbanization has resulted in an escalating increase in exposure in China. Positive human behavior, however, could directly affect both impacts and recovery time. Hence, assessing the risk perception of the inhabitants in low-lying flood-prone areas – a perspective lacking in previous researches – is an important aspect of flood-risk management (Aerts et al., 2018). And, just as in JRW, both high-income and low-income regions may benefit greatly from investing in adaption

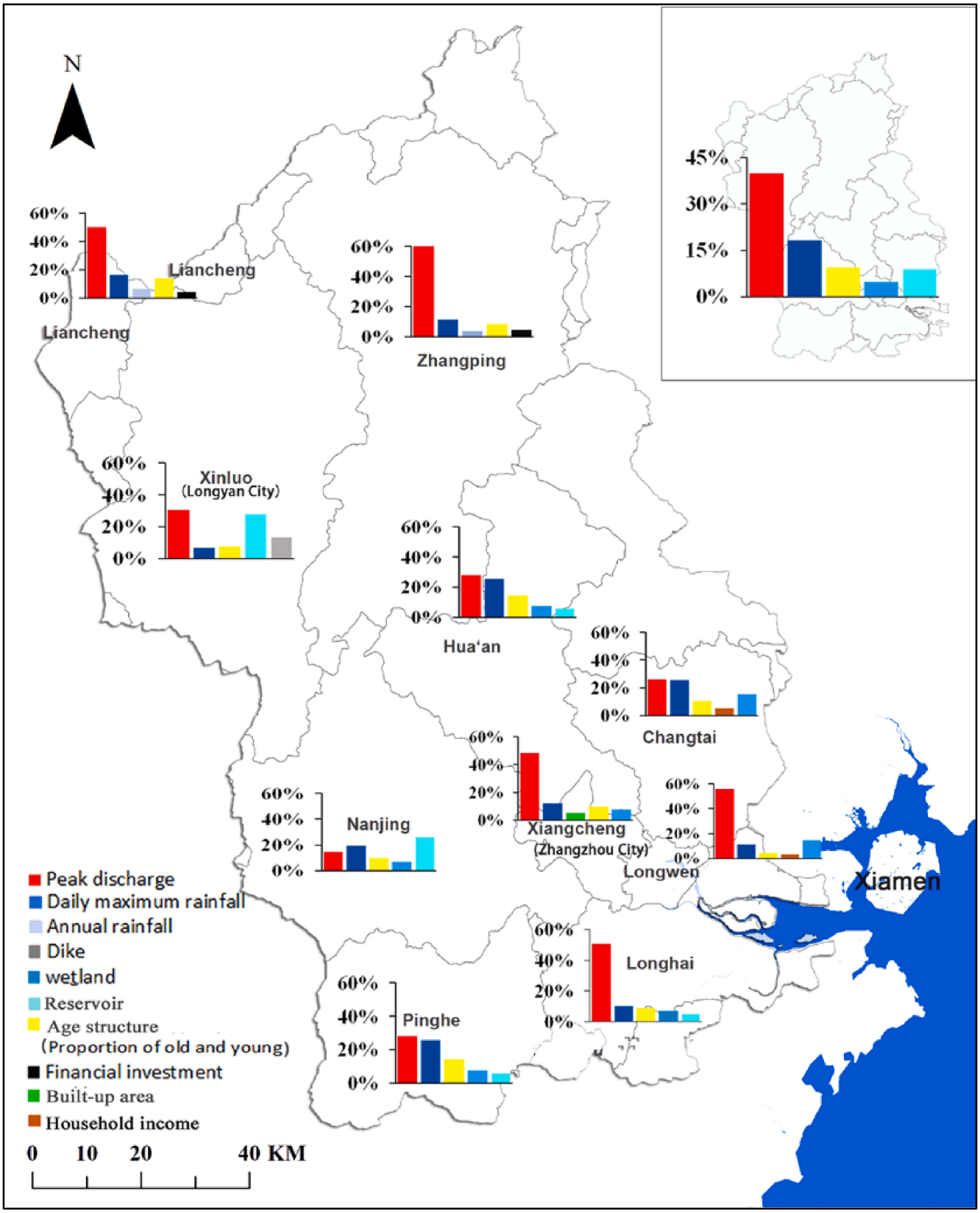

Fig. 9. Analysis of indicators whose contribution rank top 5 for the whole watershed (top right) and each district from 1991 to 2015, compared with the base year (1990).

measures (Winsemius et al., 2016), although we should also note that the flood adaptive capacity varies greatly over different regions, for various reasons (e.g., the political attitudes of decision-makers, socio-economic status), and so far, regional adaption has been lacking in the incorporation of spatially heterogeneous flood protection measures (Willner et al., 2018). Therefore, in consideration of spatio-temporal dynamics in climate change, physical and socio-economic development, policymakers should develop spatially heterogeneous adaption strategies to make the living environment more resilient to floods in the future.

4.4. Ltations

This study has several limitations that need to be improved through future research. First, to assess the flood risk more comprehensively, the roughness or more indicators need to be added to the flood risk assessment framework. Second, some indicators (e.g., electrical facilities, number of flood control offices established) for a selected year was sometimes used to represent all the periods due to the lack of data, resulting in the neglecting of the contribution of these indicators to flood risk variations.

5. Conclusion

To build a comprehensive SMCA flood assessment model in the JRW, a wide range of indicators were chosen, in the areas of meteorology, hydrology, land use, flood protection measures, socio-economic data, and human behavior. Furthermore, the flood risk variations during the period 1990 to 2015, along with the contributions of each indicator to the flood risk variation were explored. The conclusions are summarized as follows.

(1) The flood risk in the downstream stretch of the JRW was higher than that in the upstream stretch. From 1990 to 2015, looking at 5-year intervals, the highest flood risk appeared during 2006–2010, the lowest during 2011–2015
(2) The hazard component contributed the most to the flood risk variation, in most areas of the JRW, compared to the other components: exposure, sensitivity, and adaptive capacity. However, the adaptive capacity contributed the most to the flood risk variation in the Xinluo district, suggesting that the stakeholders of the Xinluo district spared no effort to reduce the flood risk, and some improvements were indeed achieved.
(3) The top 5 driving factors of flood risk evolution in JRW were: peak discharge (39.96%) > daily maximum rainfall (18.16%) > proportion of old and youth (9.55%) > dike (8.92%) > reservoir (4.75%). Furthermore, the expansion of built-up showed an obvious effect on flood risk change in Xiangcheng district (5.21%), the financial investment showed an obvious effect on flood risk change in Liancheng district (4.65%) and Zhangping district (4.55%).

The findings of this study have important implications for watershed flood risk management. (1) Policymakers should take into consideration not only the flood hazard but also exposure, sensitivity, and adaptive capacity, to assess flood risk comprehensively. (2) As human activities play a major role during flood disasters, human behavior (such as flood risk perception) should be incorporated into flood disaster risk assessment. (3) Because flood risk is spatially heterogeneous and changes dynamically, spatially heterogeneous flood protection measures should be incorporated when developing flood adaption strategies.

Declaration of Competing Interest

The authors declare that they have no known competing financial interests or personal relationships that could have appeared to influence the work reported in this paper.

Acknowledgments

This study was supported by the National Natural Science Foundation of China (41661144032), the National Natural Science Foundation of China (42007418), the National Key Research and Development Program of China (2017YFC0506603), the FJIRSM&IUE Joint Research Fund (Y8L0971), and the Fujian Provincial Natural Science Foundation (2019J05160).

Appendix A. Supplementary data

Supplementary data to this article can be found online at https://doi.org/10.1016/j.ecolind.2020.107134.

References

Aerts, J.C., 2018. A review of cost estimates for flood adaptation. Water 10 (11), 1646.
Aerts, J.C., Botzen, W.J., Clarke, K.C., Cutter, S.L., Hall, J.W., Merz, B., Kunreuther, H., 2018. Integrating human behaviour dynamics into flood disaster risk assessment. Nature Clim. Change 8 (3), 193–199.
Ali, R., Kuriqi, A., Abubaker, S., Kisi, O., 2019a. Hydrologic alteration at the upper and middle part of the yangtze river, China: towards sustainable water resource management under increasing water exploitation. Sustainability 11 (19), 5176.
Ali, R., Kuriqi, A., Abubaker, S., Kisi, O., 2019b. Long-term trends and seasonality detection of the observed flow in Yangtze River using Mann-Kendall and Sen's innovative trend method. Water 11 (9), 1855.
Ardıçlıoğlu, M., Kuriqi, A., 2019. Calibration of channel roughness in intermittent rivers using HEC-RAS model: Case of Sarimsakli creek, Turkey. SN Appl. Sci. 1 (9), 1080.
Armaş, I., Avram, E., 2009. Perception of flood risk in Danube Delta, Romania. Natural Hazards 50 (2), 269–287.
Balica, S.F., Douben, N., Wright, N.G., 2009. Flood vulnerability indices at varying spatial scales. Water Sci. Technol. 60 (10), 2571–2580.
Bodoque, J.M., Díez-Herrero, A., Amérigo, M., García, J.A., Olcina, J., 2019. Enhancing flash flood risk perception and awareness of mitigation actions through risk communication: A pre-post survey design. J. Hydrol. 568, 769–779.
Chen, Y., Liu, R., Barrett, D., Gao, L., Zhou, M., Renzullo, L., Emelyanova, I., 2015. A spatial assessment framework for evaluating flood risk under extreme climates. Sci. Total Environ. 538, 512–523.
Chau, V.N., Holland, J., Cassells, S., Tuohy, M., 2013. Using GIS to map impacts upon agriculture from extreme floods in Vietnam. Appl. Geogr. 41, 65–74.
Chang, H.S., Chen, T.L., 2016. Spatial heterogeneity of local flood vulnerability indicators within flood-prone areas in Taiwan. Environ. Earth Sci. 75 (23), 1484.
Dang, N.M., Babel, M.S., Luong, H.T., 2011. Evaluation of food risk parameters in the day river flood diversion area, Red River delta, Vietnam. Natural Hazards 56 (1), 169–194.
Field, C.B., Barros, V., Stocker, T.F., Dahe, Q., 2012. Managing the risks of extreme events and disasters to advance climate change adaptation: special report of the intergovernmental panel on climate change. Cambridge University Press.
Foudi, S., Osés-Eraso, N., Tamayo, I., 2015. Integrated spatial flood risk assessment: The case of Zaragoza. Land Use Policy 42, 278–292.
Furdada, G., Calderón, L.E., Marqués, M.A., 2008. Flood hazard map of La Trinidad (NW Nicaragua) Method and results. Natural Hazards 45 (2), 183–195.
Huang, J., Huang, Y., Zhang, Z., 2014. Coupled effects of natural and anthropogenic controls on seasonal and spatial variations of river water quality during baseflow in a coastal watershed of Southeast China. PLoS One 9 (3), e91528.
Huang, J., Pontius Jr, R.G., Li, Q., Zhang, Y., 2012. Use of intensity analysis to link patterns with processes of land change from 1986 to 2007 in a coastal watershed of southeast China. Appl. Geogr. 34, 371–384.
Jongman, B., Kreibich, H., Apel, H., Barredo, J.I., Bates, P.D., Feyen, L., Ward, P.J., 2012. Comparative flood damage model assessment: Towards a European approach. Natural Hazards Earth Syst. Sci. (NHESS) 12 (12), 3733–3752.
Jongman, B., Winsemius, H.C., Aerts, J.C., De Perez, E.C., Van Aalst, M.K., Kron, W., Ward, P.J., 2015. Declining vulnerability to river floods and the global benefits of adaptation. Proc. Natl. Acad. Sci. 112 (18), E2271–E2280.
Koks, E.E., Bočkarjova, M., de Moel, H., Aerts, J.C., 2015. Integrated direct and indirect flood risk modeling: development and sensitivity analysis. Risk Anal. 35 (5), 882–900.
Kundzewicz, Z.W., Hegger, D.L.T., Matczak, P., Driessen, P.P.J., 2018. Opinion: Flood-risk reduction: Structural measures and diverse strategies. Proc. Natl. Acad. Sci. 115 (49), 12321–12325.
Kuriqi, A., Ardiçlioglu, M., Muceku, Y., 2016. Investigation of seepage effect on river dike's stability under steady state and transient conditions. Pollack Periodica 11 (2), 87–104.
Kuriqi, A., Koçileri, G., Ardiçlioğlu, M., 2020. Potential of Meyer-Peter and Müller approach for estimation of bed-load sediment transport under different hydraulic regimes. Model. Earth Syst. Environ. 6 (1), 129–137.
Lai, C., Chen, X., Chen, X., Wang, Z., Wu, X., Zhao, S., 2015. A fuzzy comprehensive evaluation model for flood risk based on the combination weight of game theory. Natural Hazards 77 (2), 1243–1259.

Lin, T., Cao, X., Huang, N., Xu, L., Li, X., Zhao, Y., Lin, J., 2018. Social cognition of climate change in coastal community: A case study in Xiamen City, China. Ocean Coastal Manage. 104429.
Liu, R., Chen, Y., Wu, J., Gao, L., Barrett, D., Xu, T., Yu, J., 2016. Assessing spatial likelihood of flooding hazard using naïve Bayes and GIS: A case study in Bowen Basin, Australia. Stochastic Environ. Res. Risk Assessment 30 (6), 1575–1590.
Lyu, H.M., Shen, J.S., Arulrajah, A., 2018. Assessment of geohazards and preventative countermeasures using AHP incorporated with GIS in Lanzhou, China. Sustainability 10 (2), 304.
Martínez-Graña, A.M., Boski, T., Goy, J.L., Zazo, C., Dabrio, C.J., 2016. Coastal-flood risk management in central Algarve: Vulnerability and flood risk indices (South Portugal). Ecol. Indic. 71, 302–316.
Munich, R. E., 2017. Natural catastrophe losses at their highest for four years. Munich RE.
Saaty, T.L., 1977. A scaling method for priorities in hierarchical structures. J. Math. Psychol. 15 (3), 234–281.
Saaty, T.L., 2008. Decision making with the analytic hierarchy process. Int. J. Services Sci. 1 (1), 83–98.
Sadiq, R., Tesfamariam, S., 2009. Environmental decision-making under uncertainty using intuitionistic fuzzy analytic hierarchy process (IF-AHP). Stochastic Environ. Res. Risk Assess. 23 (1), 75–91.
Swiss Re., 2017. Preliminary sigma catastrophe estimates for 2017.
The Ministry of Water Resources of the People's Republic of China., 2017. China Flood and Drought Bulletin 2017. China Water Power Press, Beijing.
Thieken, A.H., Cammerer, H., Dobler, C., Lammel, J., Schöberl, F., 2016. Estimating changes in flood risks and benefits of non-structural adaptation strategies – A case study from Tyrol, Austria. Mitigation Adapt. Strategies Global Change 21 (3), 343–376.
UNISDR., 2011. Global assessment report on disaster risk reduction: Revealing risk, redefining development.
Visser, H., Petersen, A.C., Ligtvoet, W., 2014. On the relation between weather-related disaster impacts, vulnerability and climate change. Clim. Change 125 (3–4), 461–477.
Vousdoukas, M.I., Mentaschi, L., Voukouvalas, E., Bianchi, A., Dottori, F., Feyen, L., 2018. Climatic and socioeconomic controls of future coastal flood risk in Europe. Nature Clim. Change 8 (9), 776–780.
Wang, Y., Li, Z., Tang, Z., Zeng, G., 2011. A GIS-based spatial multi-criteria approach for flood risk assessment in the Dongting Lake Region, Hunan, Central China. Water Resourc. Manage. 25 (13), 3465–3484.
Willner, S.N., Levermann, A., Zhao, F., Frieler, K., 2018. Adaptation required to preserve future high-end river flood risk at present levels. Sci. Adv. 4 (1), eaao1914.
Winsemius, H.C., Aerts, J.C., Van Beek, L.P., Bierkens, M.F., Bouwman, A., Jongman, B., Ward, P.J., 2016. Global drivers of future river flood risk. Nat. Climate Change 6 (4), 381–385.
Wu, Y., Zhong, P.A., Zhang, Y., Xu, B., Ma, B., Yan, K., 2015. Integrated flood risk assessment and zonation method: A case study in Huaihe River basin, China. Natural Hazards 78 (1), 635–651.
Xiao, Y., Yi, S., Tang, Z., 2017. Integrated flood hazard assessment based on spatial ordered weighted averaging method considering spatial heterogeneity of risk preference. Sci. Total Environ. 599, 1034–1046.
Yeganeh, N., Sabri, S., 2014. Flood vulnerability assessment in Iskandar Malaysia using multi-criteria evaluation and fuzzy logic. Res. J. Appl. Sci. Eng. Technol. 8 (16), 1794–1806.